to trigger the full activation of *CLN1* and *CLN2* through the positive feedback loop.

The physiological significance of the loop is still unclear because *cln1 cln2 cln3* triple mutants kept alive by virtue of *CLN2* expressed from a constitutively expressed promoter can proliferate efficiently[2,8]. This means either that the regulation of G1 cyclins is not essential for viability or that there exists also a post-transcriptional mechanism for *CLN2*'s regulation, as there must be for *CLN3* (refs 3, 11). It is also unknown how the yeast pheromone signal transduction pathway prevents the loop from firing and how the loop is eventually turned off to make way for the formation of different forms of the CDC28 kinase (for example involving G2-specific cyclins)[14,15].

A question remains concerning the mechanism by which CDC28 kinase activity raises *CLN1* and *CLN2* transcript levels. SWI4 and SWI6, which are components of a transcription complex required for CDC28-dependent *HO* expression, are also required for CLN2 transcription. Therefore, one possibility is that phosphorylation of SWI4 and SWI6 complexes by the CDC28 protein kinase may increase their ability to activate transcription. □

Received 9 May; accepted 3 June 1991.

1. Pringle, J. R. & Hartwell, L. H. In *The Molecular Biology of the Yeast* Saccharomyces: *Life Cycle and Inheritance*. 97–142 (Cold Spring Harbor Laboratory, New York, 1981).
2. Richardson, H. E., Wittenberg, C., Cross, F. & Reed, S. I. *Cell* **59**, 1127–1133 (1989).
3. Nash, R., Tokowa, G., Anand, S., Erickson, K. & Futcher, A. B. *EMBO J.* **7**, 4335–4346 (1988).
4. Cross, F. R. *Molec. cell. Biol.* **10**, 6482–6490 (1990).
5. Wittenberg, C., Sugimoto, K. & Reed, S. I. *Cell* **62**, 225–237 (1990).
6. Stern, M., Jensen, R. & Herskowitz, I. *J. molec. Biol.* **178**, 853–868 (1984).
7. Breeden, L. & Nasmyth, K. *Cell* **48**, 389–397 (1987).
8. Nasmyth, K. A. & Dirick, L. *Cell* (in the press).
9. Cross, F., Hartwell, L. H., Jackson, C. & Konopka, J. B. *A. Rev. Cell Biol.* **4**, 429–457 (1988).
10. Nasmyth, K. A. *Cell* **63**, 1117–1120 (1990).
11. Cross, F. R. *Molec. cell. Biol.* **8**, 4675–4684 (1988).
12. Reed, S. I. *Trends Genet.* **7**, 95–99 (1991).
13. Price, C., Nasmyth, K. & Schuster, T. *J. molec. Biol.* **218**, 543–556 (1991).
14. Surana, U. *et al. Cell* **65**, 145–162 (1991).
15. Ghiara, J. B. *et al. Cell* **65**, 163–174 (1991).
16. Nasmyth, K. A. *Nature* **302**, 670–676 (1983).
17. Nasmyth, K. *Cell* **42**, 225–235 (1985).
18. Andrews, B. J. & Herskowitz, I. *Nature* **342**, 803–833 (1989).
19. Nasmyth, K. A., Adolf, G., Lydall, D. & Seddon, A. *Cell* **62**, 631–647 (1990).

Acquired immunity and epidemiology of *Schistosoma haematobium*

M. E. J. Woolhouse*, P. Taylor†, D. Matanhire‡ & S. K. Chandiwana‡

* Department of Zoology, University of Oxford, South Parks Road, Oxford OX1 3PS, UK
† Training Centre for Water and Sanitation, University of Zimbabwe, PO Box MP167, Harare, Zimbabwe
‡ Blair Research Laboratory, PO Box 8105, Causeway, Harare, Zimbabwe

HUMAN immune responses to schistosome infection have been characterized in detail[1–5]. But there has been controversy[6] over the relative importance of ecological factors (variation in exposure to infection) and immunological factors (acquired immunity) in determining the relationships between levels of infection and age typically found in areas where infection is endemic[7,8]. Independent effects of exposure and age on the rates of reinfection with *Schistosoma haematobium* after chemotherapy have been demonstrated in the Gambia[9] and Zimbabwe[8]. This age effect could be the result of acquired immunity to infection. Indeed, allowing for variation in exposure and age, low rates of reinfection in the Gambia are correlated with high amounts of specific IgE antibodies[10]—human IgE can kill *S. mansoni* schistosomulae *in vitro*[11]. Further, animals can acquire immunologically mediated resistance to *S. mansoni* infection[12–14], although nonimmunological factors could also be involved[15]. Acquisition of this immunity seems to be related to the cumulative effects of repeated infection and provides only partial protection[12,13,16]. These characteristics are consistent with immuno-epidemiological data for both *S. mansoni* and *S. haematobium* infections of humans[4,17]. We have now analysed age–prevalence data for human infection with *S. haematobium*, and find patterns of variation that are indeed consistent with the epidemiological effects of acquired immunity predicted by mathematical models.

The epidemiological effects of an immune response to schistosome infection can be investigated using a mathematical model developed by Anderson and colleagues[18,19]. This is an age-structured immigration–death model that considers changes with age, a, in the mean intensity of infection (number of adult schistosomes), $m(a)$, as a function of the per capita rate of infection, Λ, and the per capita parasite mortality rate, γ. Acquired immunity moderates the rate of parasite establishment. The model predicts the following consequences of a higher rate of infection, Λ, on endemic epidemiological patterns: (1) an increase in the convexity of the age–intensity curve; (2) an increase in the peak intensity of infection, $m(a^*)$; and (3) for certain parameter values, a decrease in the age of peak intensity of infection, a^*. The last two of these imply a negative correlation between $m(a^*)$ and a^* for populations with different values of Λ (Fig. 1). These predictions hold even if Λ is itself age-dependent, perhaps owing to age-related variation in exposure, provided that the form of the relationship does not vary systematically between populations subject to high or low

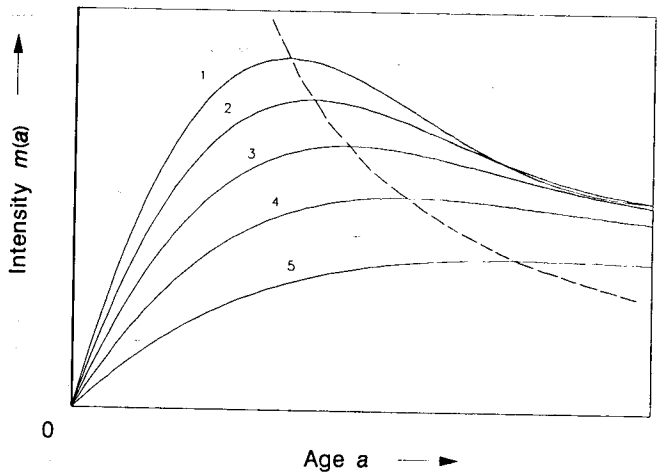

FIG. 1 Predicted patterns for age-related changes in the intensity of infection using a version of the model of Anderson and colleagues[18,19]. The model considers changes in the mean intensity of infection, m, with respect to age, a. For certain parameter values (see below) the model predicts an age-intensity curve of the form:

$$m(a) = A + e^{-(\gamma+\sigma)a/2}[2\Lambda \sin(a\theta/2)[1 - A(\gamma+\sigma)/2\Lambda]/\theta - A\cos(a\theta/2)] \quad (1)$$

with $A = \Lambda\sigma/(\sigma\gamma + \nu\Lambda)$ and $\theta = [4\nu\Lambda - (\gamma-\sigma)^2]^{1/2}$, where Λ is the per capita rate of infection, ν is a measure of the decrease in the per capita rate of parasite establishment due to acquired immunity, σ is the rate of loss of immunological memory, and γ is the per capita mortality rate for adult parasites. The parameter Λ is a function of the mean per capita fecundity of adult parasites, intermediate host snail population density, life expectancy of infected snails, human population density, per capita rate of infection of snails per adult parasite and per capita rate of infection of humans per infected snail. The rates of infection of both humans and snails are functions of the mean water contact rate of the human population. Equation (1) applies where parameter values satisfy the condition $4\nu\Lambda > (\gamma-\sigma)^2$. The solid curves in the figure represent equilibrium age-intensity curves predicted by equation (1) with parameter values $\nu = 0.0015$, $\sigma = 0.04$, $\gamma = 0.027$ throughout and $\Lambda = 2.2$, 1.8, 1.4, 1.0 and 0.6 for curves labelled 1–5, respectively. The shift in the predicted peak intensity of infection, $m(a^*)$ with the predicted age of peak intensity, a^*, is shown by the broken curve. This relationship is generated solely by variation in Λ.

transmission, that is, if $d\Lambda/da$ is independent of Λ (see below). The model formalizes earlier precictions based on verbal arguments[20].

Variations in age-intensity patterns for human infection with schistosomes[20,21] and hookworm[19] have been reported to be consistent with these predictions, but a robust analysis has not been possible owing to the lack of suitable field data. We have analysed 17 data sets recording the prevalence within age groups, $P(a)$, of *S. haematobium* infection for more than 2,000 children in Zimbabwe. There is a statistically significant negative correlation between $P(a^*)$ and a^* across these data sets (Fig. 2). The relationship between prevalence, P, and m depends on the distribution of schistosomes among hosts (the more aggregated this distribution, the lower P is for a given m), so the pattern shown in Fig. 2 could reflect differences in the parasite distribution rather than in mean intensities of infection. But available data indicate that the degree of aggregation, as indexed by the variance-to-mean ratio for egg counts, does not increase with age (Fig. 3), so the pattern of Fig. 2 must reflect differences in $m(a^*)$.

The observed pattern is therefore consistent with model predictions. The only other interpretation possible is that there is a relationship between Λ and age, perhaps due to age-related variation in exposure, such that populations with high overall Λ also tend to have peak values of Λ at an earlier age. None of the many epidemiological and sociological studies carried out in Zimbabwe indicates such a relationship[22,23].

Although the analysis captures the essentials of the dynamic interaction between infection and acquired immunity, it ignores certain features. We have not considered the effects of blocking antibodies, which are thought to be involved in human schistosome infection, or age-dependency in the immune response

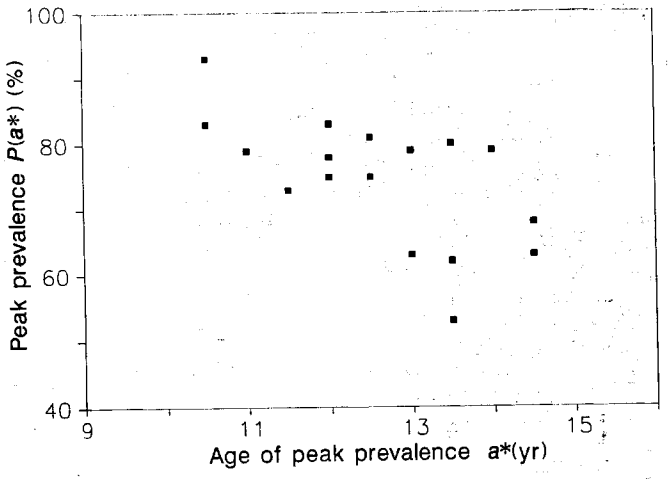

FIG. 2 Relationship between peak prevalence of infection, $P(a^*)$, and age of peak prevalence, a^*, for *S. haematobium* infections of school-children in Zimbabwe. Data are from 17 primary schools in the Zimbabwe highveld. A total of 2,185 children between 6 and 16 years old were screened for infection by examination of a 10-ml urine sample[26,27]. Data from adjacent one-year age classes have been pooled where necessary to provide estimates of $P(a^*)$ based on more than 20 individuals. In no case where data were available from additional age classes (six schools) was peak prevalence observed outside the age range 6–16 years. The schools were located within an area ~100 × 100 km and represent contiguous populations within a geographically, culturally and sociologically homogeneous region[26,27] (compare with refs 19 and 21). Several factors may contribute to variation in the per capita rates of infection experienced by these different populations: differences in human population densities, differences in population densities of the intermediate host snails (*Bulinus globosus*), and differences in mean water contact rates (reflecting differences in the availability and convenience of natural water bodies). The relationship between $P(a^*)$ and a^* is in the direction predicted by the model incorporating acquired immunity (Fig. 1) and is statistically significant: Kendall's rank correlation $\tau = -0.438$, $n = 17$, $P < 0.01$ (one-tailed test).

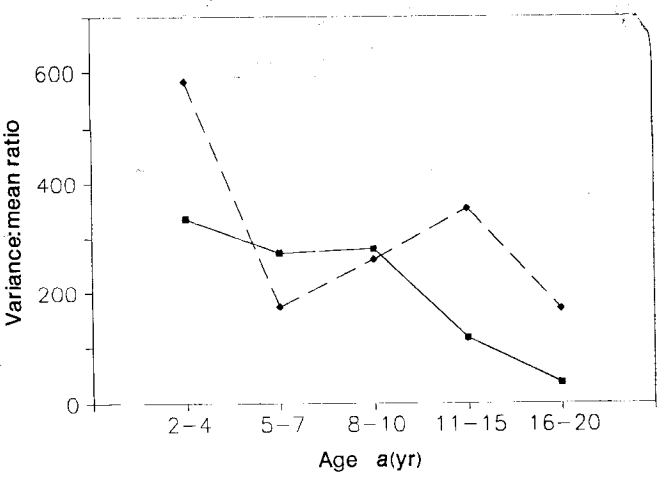

FIG. 3 Relationships between the variance-to-mean ratio for intensity of *S. haematobium* infections and age. The data are egg counts per 10 ml urine (single sample) from children between 6 and 20 years old, divided into five age classes. ■, Sample of 237 children from a community in eastern Zimbabwe[8]. ◆, Sample of 188 children from a community in the Zimbabwe highveld (S.K.C. and M.E.J.W., unpublished data). Kendall's rank correlation $\tau = -0.800$ ($P = 0.04$) and -0.400 ($P = 0.24$), respectively. Peak levels of infection occur among 8–10-year-old children in both samples.

itself[24]. More information is needed before these effects can be incorporated in mathematical models. Nor have we considered the effects of acquired immunity on schistosome mortality and fecundity and on the fraction of eggs passed out of the host's body, effects which have been reported in animal models[13,25]. Because egg output is the most widely used index of the intensity of infection in humans, any effects of acquired immunity on egg output need to be better understood if immuno-epidemiological data are to be interpreted correctly.

In conclusion, we have shown patterns of variation in age-prevalence data for human infection with *S. haematobium* that are consistent with current understanding of the epidemiological effects of acquired immunity. To our knowledge, such a relationship has not previously been demonstrated for any human macroparasite infection. The interaction between schistosome infection and acquired immune responses are complex and we expect that mathematical models will prove valuable for the interpretation of field data. □

Received 22 March; accepted 24 April 1991.

1. Sturrock, R. F. *et al. Trans. R. Soc. trop. Med. Hyg.* **77,** 363–371 (1983).
2. Butterworth, A. E. *et al. Trans. R. Soc. trop. Med. Hyg.* **79,** 393–408 (1985).
3. Butterworth, A. E. *et al. Parasitology* **94,** 281–300 (1987).
4. Hagan, P. *et al. Trans. R. Soc. trop. Med. Hyg.* **81,** 938–946 (1987).
5. Dunne, D. W. *et al. Eur. J. Immun.* **18,** 123–131 (1988).
6. Wilkins, H. A. in *Biology of Schistosomes* (eds Rollinson, D. & Simpson, A. J. G) 379–398 (Academic, London, 1987).
7. Wilkins, H. A., Goll, P. H., Marshall, T. F. & Moore, P. J. *Trans. R. Soc. trop. Med. Hyg.* **78,** 216–221 (1984).
8. Chandiwana, S. K., Woolhouse, M. E. J. & Bradley, M. *Parasitology* **102,** 73–83 (1991).
9. Wilkins, H. A., Blumenthal, U. J., Hagan, P., Hayes, R. J. & Tulloch, S. *Trans. R. Soc. trop. Med. Hyg.* **81,** 29–35 (1987).
10. Hagan, P., Blumenthal, U. J., Dunn, D., Simpson, A. J. G. & Wilkins, H. A. *Nature* **349,** 243–245 (1991).
11. Capron, A., Dessaint, J. P., Capron, M., Ouma, J. H. & Butterworth, A. E. *Science* **238,** 1065–1072 (1987).
12. Smithers, S. R. & Terry, R. J. *Trans. R. Soc. trop. Med. Hyg.* **61,** 517–533 (1967).
13. Dean, D. A. *Expl Parasit.* **55,** 1–104 (1983).
14. Pearce, E. J. & McLaren, D. J. *Parasitology* **87,** 465–479 (1983).
15. Wilson, R. A. *Parasit. Today* **6,** 354–358 (1990).
16. James, S. L. & Cheever, A. W. *Parasitology* **91,** 301–315 (1985)
17. Hagan, P. in *Biology of Schistosomes* (eds Rollinson, D. & Simpson, A. J. G) 295–320 (Academic, London, 1987).
18. Crombie, J. A. & Anderson, R. M. *Nature* **315,** 491–493 (1985).
19. Anderson, R. M. & May, R. M. *Nature* **315,** 493–496 (1985).
20. Clarke, V. de V. *C. Afr. J. Med.* **12,** Suppl., 1–30 (1966).
21. Anderson, R. M. in *Clincial Tropical Medicine and Communicable Diseases* Vol. 2 (ed. Mahmoud, A. A. F.) 279–300 (Bailliere Tindall, London, 1987).
22. Chandiwana, S. K. *Soc. Sci. Med.* **25,** 495–505 (1987).
23. Chandiwana, S. K. & Christensen, N. O. *Trop. med. Parasit.* **39,** 187–193 (1988).
24. Butterworth, A. E. & Hagan, P. *Parasit. Today* **3,** 11–16 (1987).

5. Doenhoff, M. J., Hassounah, O., Murare, H., Bain, J. & Lucas, S. *Trans. R. Soc. trop. Med. Hyg.* **80**, 503–514 (1986).
26. Taylor, P., Chandiwana, S. K. & Matanhire, D. *Acta Trop.* **47**, 91–100 (1990).
27. Taylor, P., Chandiwana, S. K. & Matanhire, D. *Community Based Schistosomiasis Control in Zimbabwe* (IDRC, Canada, in the press).

ACKNOWLEDGEMENTS. We thank R. M. Anderson, A. E. Butterworth, R. D. Gregory, P. Hagan, A. E. Keymer, A. R. McLean & H. A. Wilkins for discussions. This work was supported by the International Development Research Centre, Canada, and a Beit Memorial Fellowship for Medical Research (M.E.J.W.).

Activation of *Escherichia coli* prohaemolysin to the mature toxin by acyl carrier protein-dependent fatty acylation

Jean-Paul Issartel, Vassilis Koronakis & Colin Hughes

Department of Pathology, University of Cambridge, Tennis Court Road, Cambridge CB2 1QP, UK

HAEMOLYSIN secreted by pathogenic *Escherichia coli* binds to mammalian cell membranes, disrupting cellular activities and lysing cells by pore-formation. It is synthesized as nontoxic prohaemolysin (proHlyA), which is activated intracellularly by a mechanism dependent on the cosynthesized HlyC. Haemolysin is one of a family of membrane-targeted toxins, including the leukotoxins of *Pasteurella* and *Actinobacillus* and the bifunctional adenylate cyclase haemolysin of *Bordetella pertussis*, which require this protoxin activation[1–5]. HlyC alone cannot activate proHlyA, but requires a cytosolic activating factor[6]. Here we report the cytosolic activating factor is identical to the acyl carrier protein and that activation to mature toxin is achieved by the transfer of a fatty acyl group from acyl carrier protein to proHlyA. Only acyl carrier protein, not acyl-CoA, can promote HlyC-directed proHlyA acylation, but a range of acyl groups are effective.

In vitro post-translational activation of proHlyA to the haemolytically active toxin is achieved by mixing cell extracts containing separately the proHlyA of relative molecular mass 110,000 (M_r 110K) and the 19.8K HlyC, but activation is lost when both proteins are purified[6]. Activation is recovered by addition of an *E. coli* cell extract, demonstrating the existence of an essential cytosolic activating factor (CAF)[6]. Purification of the protease-sensitive CAF increased about 120-fold in the specific proHlyA-activating activity (Fig. 1*a*, *b*). Anion exchange chromatography revealed that CAF is highly negatively charged and gel filtration indicated that it has an M_r of 9–10K (Fig. 1*a*). SDS-PAGE showed a single polypeptide (Fig. 1*b*, lanes 1–3) migrating as a diffuse, weakly stained band with a higher apparent M_r of 16–19K. N-terminal sequencing of purified CAF showed that the first 20 amino acids (Fig. 1*c*) are identical to those of *E. coli* acyl carrier protein (ACP), an 8.86K negatively charged polypeptide which, like CAF, migrates abberantly during SDS-PAGE[7,8] (Fig. 1*b*, lane 4).

In *E. coli*, ACP can function either in the unacylated form, as in the synthesis of periplasmic glucans[9], or in the acylated form, donating acyl residues linked by a thioester bond to the covalently bound phosphopantotheine group, for example in lipid biosynthesis. That proHlyA activation requires acyl-ACP was indicated by the loss of CAF activity after treatment with hydroxylamine, dithiothreitol (DTT) or $NaBH_4$ (not shown), each of which hydrolyses thioester linkages[10] between acyl groups and holo-ACP (ACP—SH). Further evidence was based on the characteristic behaviour of ACP—SH and acyl-ACP during chromatography in octyl sepharose. Although ACP—SH does not bind to this medium the acyl-ACP adsorbs tightly until eluted by 2-propanol[11]. Purified CAF adsorbed to octyl sepharose, and when eluted by 2-propanol it was able to activate proHlyA in the presence of HlyC (Table 1, bound fraction).

TABLE 1 Binding of CAF to octyl sepharose

	Preacylation (HU)	Postacylation (HU)
CAF	1.2×10^3	1.1×10^5
Unbound fraction	2.0	2.7×10^4
Bound fraction	0.6×10^3	0.9×10^4

A 100 μl aliquot of CAF (purified as in Fig. 1) able to generate 1.2×10^3 HUs was mixed with 20 μl octyl sepharose CL4B (Pharmacia). After incubation for 10 min at 22 °C, the chromatographic medium was pelleted by centrifugation and the supernatant withdrawn (the 'unbound fraction'), the pellet was then mixed with 100 μl HED buffer containing 25% 2-propanol. The supernatant obtained after centrifugation of this was the 'bound fraction'. Both fractions were assayed for proHlyA activation before and after enzymatic acylation (pre- and postacylation, respectively), and the activities expressed in HUs, standardized to 100 μl of the original fractions. Enzymatic acylation was performed essentially as recommended[11]; aliquots of purified CAF, unbound fraction and bound fraction were lyophilized and incubated with 160 μM myristic acid (sodium salt) and 0.8 mU acyl-ACP synthetase (Sigma) in 20 μl. After 30 min at 37 °C the proHlyA activation competence of the samples was assayed. *In vitro* activation of proHlyA in the presence of HlyC and the CAF-containing samples was performed as described[6]. Routinely, purified proHlyA (6 μg) was preincubated for 10 min at 22 °C in the presence of 80 ng purified HlyC and different amounts of CAF in a total of 50 μl HED buffer. Haemolytic activities were assayed by diluting the reaction mixes with 1 ml saline buffer, 150 mM NaCl, 20 mM $CaCl_2$ containing 2% (v/v) equine erythrocytes. After 30 min at 42 °C debris was cleared by centrifugation, and the haemoglobin released by erythrocyte lysis was read at 543 nm. One HU is defined as the amount of active HlyA promoting the release of 1 nmol haemoglobin per h.

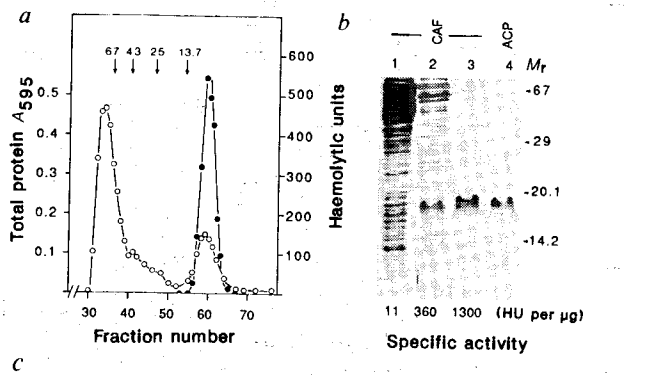

c

NH_2- ser-thr-ile-glu-glu-arg-val-lys-lys-ile-ile-gly-glu-gln-leu-gly-val-lys-gln-glu-

FIG. 1 Identity of the cytosolic activating factor (CAF) with acyl carrier protein (ACP). *a*, Final purification step of CAF through a G75 Sephadex column; protein elution profile (○), proHlyA activation in haemolytic units (●). Arrows correspond to the elution volumes of M_r markers ($M_r\times10^{-3}$). *b*, Analysis by 20% SDS-PAGE. Lanes 1, cytosolic extract 30 μg; 2, active fractions from Q sepharose chromatography 15 μg; 3, active fractions from G75 Sephadex 9 μg; 4, ACP (Sigma) 6 μg. Specific CAF activities are given as HU per μg protein. *c*, The N-terminal amino-acid sequence of purified CAF obtained by an Applied Biosystems 477A Protein Sequencer after electroblotting onto Problott membrane.

METHODS. *E. coli* strain PR7 was grown in aerated 2TY medium at 37 °C up to an absorbance at 600 nm of 1.6. Peletted cells (10,000*g*, 10 min) were resuspended in 1/20 original culture volume then disrupted in a French Press (12,000 p.s.i). Lysate was centrifuged (30,000*g*, 15 min) and 10 ml supernatant were loaded on a Q sepharose fast-flow anion exchange chromatography column (Pharmacia, 10 ml), equilibrated in 25 mM HEPES buffer, pH 8.0, 5 mM EDTA, 1 mM DTT (HED buffer). The column was washed with 50 ml HED containing 50 mM NaCl and elution was achieved using a linear 50–500 mM NaCl gradient in 250 ml HED. CAF was assayed by *in vitro* HlyC-dependent activation of proHlyA, as described in the legend to Table 1. Active fractions eluted close to 300 mM NaCl were lyophilized, solubilized with 3 ml HED containing 3 mM magnesium acetate and 70 mM NaCl and loaded on a G75 Sephadex superfine column (Pharmacia, 1.5 × 90 cm) equilibrated in the same buffer. Flow rate was 8 ml h^{-1} and 2 ml fractions were collected. Proteins were assayed either with a Coomassie-blue staining solution (*a*) or the more accurate microBCA assay (Pierce) (*b*).

TABLE 2 Activity of specific acylated forms of ACP in the activation *in vitro* of proHlyA

Fatty acid	None	C_{12}	C_{14}	C_{16}	$C_{16:1}$	$C_{18:1}$
Specific activity (HU μg^{-1})	6	1.5×10^4	7.6×10^4	2.7×10^4	3.8×10^4	0.7×10^4
Relative activity	—	0.20	1.0	0.36	0.50	0.09

HlyC-dependent proHlyA activation by ACP (Sigma) enzymatically acylated by various fatty acids, as described in Table 1. ACP (15 μM) was incubated with 160 μM fatty acid (sodium salt) and 1.5 mU acyl-ACP synthetase (Sigma) in 40 μl, at 37 °C for 30 min. Reaction mixes were diluted 500-fold and aliquots were assayed for proHlyA activation as described in Table 1. Haemolytic activities were corrected to take into account that the yields of acylated ACPs are dependent on the nature of the fatty acid used as a substrate. Accordingly, HUs were multiplied by the following correcting factors drawn from the published data[11]; C_{12} (lauric acid) = 2.2; C_{14} (myristic acid) = 1.1; C_{16} (palmitic acid) = 1.0; $C_{16:1}$ (*cis*-9-hexadecenoic acid/palmitoleic acid) = 1.8; $C_{18:1}$ (*cis*-11-octadecenoic acid/*cis*-vaccenic acid) = 2.0. Corrected specific haemolytic activities given in the table were used to define the relative ability of the different acylated-ACP to activate proHlyA, taking C_{14}-ACP as a reference.

The unbound fraction was unable to activate proHlyA, but could be converted into the activating form by *E. coli* acyl-ACP synthetase, which catalyses the ligation of fatty acids to ACP—SH in the presence of ATP-Mg^{2+}. This enzymatic acylation resulted in about a 10^4-fold increase in proHlyA activation. CAF and the octyl sepharose-bound fraction were also enhanced, but by 92-fold and 15-fold, respectively. The data suggest that purified CAF contains both acyl-ACP and ACP—SH, and that proHlyA activation requires acyl-ACP. The requirement is strict; neither acyl-CoAs nor free fatty-acids promoted activation. Commercial ACP (ACP—SH) supported low amounts of HlyC-dependent proHlyA activation (specific activity 6 haemolytic units (HU) μg^{-1}; compare with CAF 1,300 HU μg^{-1}). After enzymatic acylation with a range of fatty acids (C_{12} to $C_{18:1}$), the resulting acylated ACPs all had a specific activity about 10^4-fold higher than ACP—SH (Table 2), with myristoylated ACP the most active. Myristic acid is not as abundant in *E. coli* as palmitic, palmitoleic and *cis*-vaccenic acids, so myristoyl-HlyA may be the most active acylated toxin among a mixture secreted by the cell.

We demonstrated directly that activation involves transfer of the acyl group from acyl-ACP to proHlyA by using enzymatically synthesized [^{14}C]palmitoyl-ACP. *In vitro* activation to the haemolytic HlyA occurred concomitantly with the radiolabelling of proHlyA, that is by covalent acylation with the [^{14}C]palmitoyl group (Fig. 2*b*, lane 2). No stable intermediate fatty-acyl-HlyC was found. No activation and no radiolabelling of proHlyA occurred in the absence of HlyC (Fig. 2*b*, lane 1).

Acylation is involved in the maturation of many proteins of both prokaryotic and eukaryotic cells, including viral oncogene products, but it is achieved by various mechanisms differing according to the fatty acid transferred, the amino acid modified, and the fatty acyl donor[12]. Myristic and palmitic acids are the most common fatty acids cross-linked to proteins. Myristic acid is attached through an amide linkage to an N-terminal glycine by the specific enzyme *N*-myristoyl transferase[10,13], but acylation can also occur on internal cysteine or threonine residues (S- and O-ester linkages), and probably also lysines (amide linkage) in processes which do not show strong selectivity for specific fatty acids[12]. Fatty acyl-CoAs act as donors in both myristoylation and ester-type acylation. A further hydrophobic modification of eukaryotic proteins is the covalent attachment of glycolipid to the C-terminus of protein (glypiation)[14], whereas lipoproteins sorted to the bacterial outer membrane (for example penicillinase and pullulanase) undergo complex processing in which an *N*-acyl diglyceride cysteine is generated at the N-terminus, using fatty acids derived from phospholipids[15]. The acylation of proHlyA does not equate to any of these characterized examples.

The linkage of the radiolabelled fatty-acid group to active haemolysin (HlyA) was resistant to hydroxylamine (not shown), indicating an amide linkage. Acylation of one or more amino groups in proHlyA would explain the increased negative charge of activated HlyA, compared with proHlyA[16]. An N-terminal proHlyA acylation similar to *N*-myristoylation seems impossible as there is no specificity for a myristoyl group, nor for the N-terminal sequence as the first amino acid of proHlyA is not glycine and a mutant of proHlyA lacking the N-terminal 15K is still activated[17]. More likely, fatty acylation of proHlyA involves internal amide-linkage (lysine modification), as described for the mouse nicotinic acetylcholine receptor[18], the human insulin receptor[19] and the immunoglobulin heavy-chain polypeptide of mouse B lymphocytes[20]. Internal proHlyA modification is also consistent with the isolation of a monoclonal antibody which recognizes only the active HlyA, specifically epitope 626–726[17].

Cellular fatty acylation can be central to signal transduction, protein–protein interactions, and protein anchoring to membranes[12]. Post-translational modification of proHlyA is not a requirement for HlyB-dependent secretion of HlyA, but it remains possible that it may modulate the kinetics of translocation across the two bacterial membranes. Note that where the exported substrates of eukaryotic homologues of the *E. coli* HlyB translocator are known, they are lipophilic drugs (exported

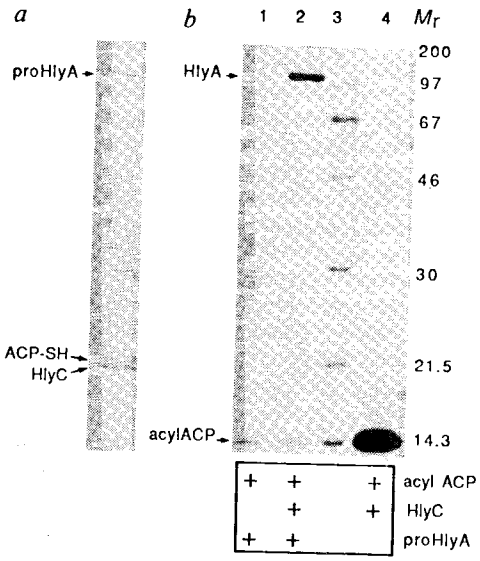

FIG. 2 Activation to the mature toxin occurs concomitantly with the transfer of radiolabelled palmitic acid from ACP to proHlyA. *a*, Coomassie blue-stained SDS-PAGE of reaction mixture components HlyC (2 μg), proHlyA (1 μg) and ACP—SH (3 μg). *b*, Fluorography of *in vitro* radiolabelling reaction mixtures containing the three components, [^{14}C]palmitoyl-ACP, proHlyA and HlyC, as shown in the box (lanes 1, 2, 4). Lane 3 shows ^{14}C-labelled M_r standards ($M_r \times 10^{-3}$).

METHODS. ACP (6 μg, Sigma) was acylated as described in the legend to Table 1 by 1.5 mU acyl-ACP synthetase in 40 μl, for 1 h at 37 °C, in the presence of 100 μM U[^{14}C]palmitic acid (sodium salt; specific radioactivity 839 mCi $mmol^{-1}$, Amersham). Then, HlyC was added to 5 μg, proHlyA to 14 μg, and incubations were performed for 30 min at 22 °C in a total volume of 120 μl. Samples (10 μl) were precipitated by 50%(v/v) ethanol (lanes 1 and 2) or 10% TCA (the control, lane 4) and pellets dissolved in SDS-PAGE loading buffer before separation on a 12.5% gel, fluorography and 2 days exposure. Note acyl-ACP migrates faster than ACP—SH, and acyl-ACP is poorly precipitated by 50% ethanol so precipitation was achieved with TCA to maximize recovery in the control lane 4.